BIOCHEMISTRY
including biophysical chemistry & molecular biology

Article

pubs.acs.org/biochemistry

Regulation of *Mycobacterium tuberculosis* D-3-Phosphoglycerate Dehydrogenase by Phosphate-Modulated Quaternary Structure Dynamics and a Potential Role for Polyphosphate in Enzyme Regulation

Xiao Lan Xu[†] and Gregory A. Grant*[,†,‡]

[†]Department of Developmental Biology and [‡]Department of Medicine, Washington University School of Medicine, 660 South Euclid Avenue, Box 8103, St. Louis, Missouri 63110, United States

Supporting Information

ABSTRACT: D-3-Phosphoglycerate dehydrogenase (PGDH) catalyzes the first reaction in the "phosphorylated" pathway of L-serine biosynthesis. In *Mycobacterium tuberculosis*, it is a type 1 enzyme (*mt*PGDH) in that it contains both an ACT domain and an ASB domain in addition to a catalytic domain. The published crystal structures (Protein Data Bank entries 1YGY and 3DC2) show a tartrate molecule interacting with cationic residues at the ASB−ACT domain interfaces and a serine molecule bound at the ACT domain interface. These sites have previously been shown to be involved in the mechanism of serine and substrate inhibition of catalytic activity. This investigation has revealed a mechanism of allosteric quaternary structure dynamics in *mt*PGDH that is modulated by physiologically relevant molecules, phosphate and polyphosphate. In the absence of phosphate and polyphosphate, the enzyme exists in equilibrium between an inactive dimer and an active tetramer that is insensitive to inhibition of catalytic activity by L-serine. Phosphate induces a conversion to an active tetramer and octamer that are sensitive to inhibition of catalytic activity by L-serine. Small polyphosphates (pyrophosphate and triphosphate) induce a conversion to an active dimer that is insensitive to L-serine inhibition. The difference in the tendency of each respective dimer to form a tetramer as well as slightly altered elution positions on size exclusion chromatography indicates that there is likely a conformational difference between the serine sensitive and insensitive states. This appears to constitute a unique mechanism in type 1 PGDHs that may be unique in pathogenic *Mycobacterium* species and may provide the organisms with a unique metabolic advantage.

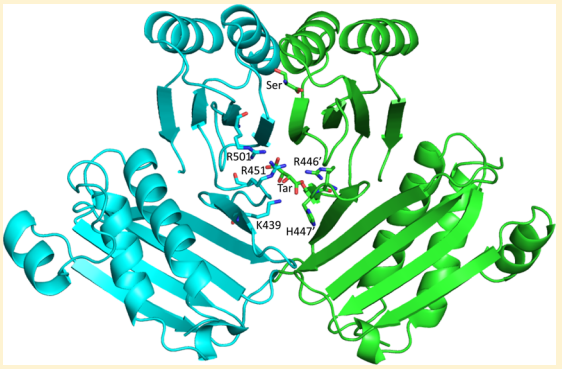

D-3-Phosphoglycerate dehydrogenase (PGDH, EC 1.1.1.95) catalyzes the first reaction in the "phosphorylated" pathway of L-serine biosynthesis in bacteria, plants, and animals by converting the glycolytic intermediate, D-3-phosphoglycerate, to phosphohydroxypyruvate (PHP).[1−6] Three types of PGDH that differ in their domain makeup have been identified.[5−7] All three types have homologous catalytic domains; however, the type 1 and type 2 PGDH enzymes contain additional structural domains, while the type 3 enzymes do not. Type 1 PGDHs contain both ACT and ASB domains, and type 2 PGDHs contain only an additional ACT domain. ACT domains are found in many metabolic enzymes and regulate catalytic activity mainly by binding amino acids and in some instances metal ions.[7] ASB domains have so far been found in only a few proteins and appear to be second, noncatalytic sites for substrate binding that function in the allosteric regulation of activity.[9−11] However, ASB domains found in vertebrate PGDHs appear to be nonfunctional.

PGDH from *Mycobacterium tuberculosis* (*mt*PGDH) is a type 1 PGDH that displays significant substrate inhibition with PHP that is not observed with the type 2 PGDH from *Escherichia coli* (*ec*PGDH).[6] It was previously shown that the degree of substrate inhibition of *mt*PGDH decreased with an increasing concentration of phosphate buffer,[8] which at the time it was first observed was attributed to an ionic strength effect as had been reported for rat PGDH (*rn*PGDH).[12] The kinetic mechanisms of both *mt*PGDH and *ec*PGDH were determined to be ordered bi-bi, but with NADH binding first with *ec*PGDH and PHP binding first with *mt*PGDH.[13,14] Inhibition by the first substrate to bind to *mt*PGDH (PHP) is inconsistent with the classical interpretations of uncompetitive substrate inhibition in an ordered bi-bi system (Scheme 1) but is consistent with competitive substrate inhibition at the active site (Scheme 2) or with an allosteric substrate inhibition model (Scheme 3).[9]

The available crystal structures of *mt*PGDH [Protein Data Bank (PDB entries 1YGY, 3DC2, and 3DDN)] were all

Received: April 17, 2014
Revised: June 2, 2014
Published: June 23, 2014

dx.doi.org/10.1021/bi500469d | *Biochemistry* 2014, 53, 4239−4249

Scheme 1

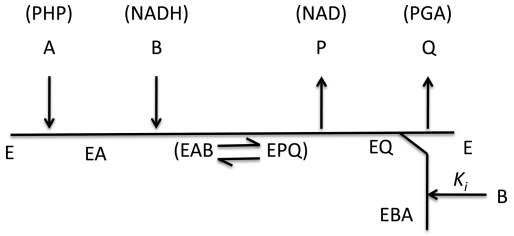

Scheme 2

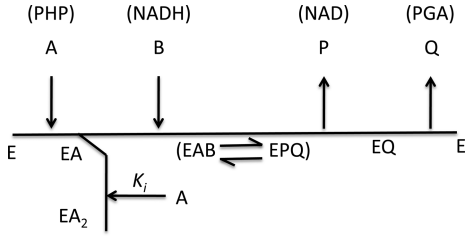

Scheme 3

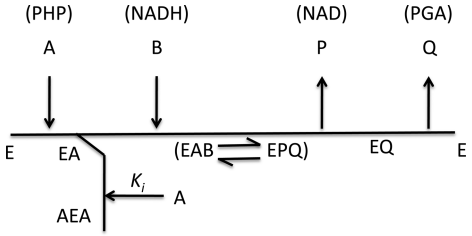

obtained in 0.1 M MES buffer (pH 6.5) containing 1 M tartrate and show a molecule of tartrate bound to a group of cationic residues at the interface between ASB and ACT domains in adjacent subunits (Figure 1).[14,15] Because tartrate is a structural analogue of the substrate and/or product of PGDH (phosphoglycerate/phosphohydroxypyruvate), it was suggested that this was a second, allosteric site for substrate binding. Subsequent investigation supported this idea and also showed that binding of the substrate to this site could be competitively weakened by NADH,[9] which is also a coenzyme for PGDH. This was consistent with stopped-flow data that showed that NADH bound to a second site on the enzyme,[14] but at the time, the binding of NADH to this site was unanticipated and not completely understood.

This investigation is a more detailed study of the role of phosphate in modulating enzyme activity and serine inhibition. Negatively charged ions, such as phosphate and polyphosphates, have the potential to bind at the ASB−ACT cationic pocket. The result of this investigation shows that many of the properties of *mt*PGDH are the result of a mechanism of allosteric regulation by quaternary structure dynamics that is modulated by phosphate ion. The results also reinforce the conclusion that the substrate inhibition seen with PHP is due mainly to an allosteric mechanism in which the substrate binds at the ASB−ACT domain interface. In addition, short polyphosphate molecules were found to have specific differential effects on the activity and ability of serine to inhibit catalytic activity. This observation suggests a possible role for polyphosphates in the regulation of this enzyme.

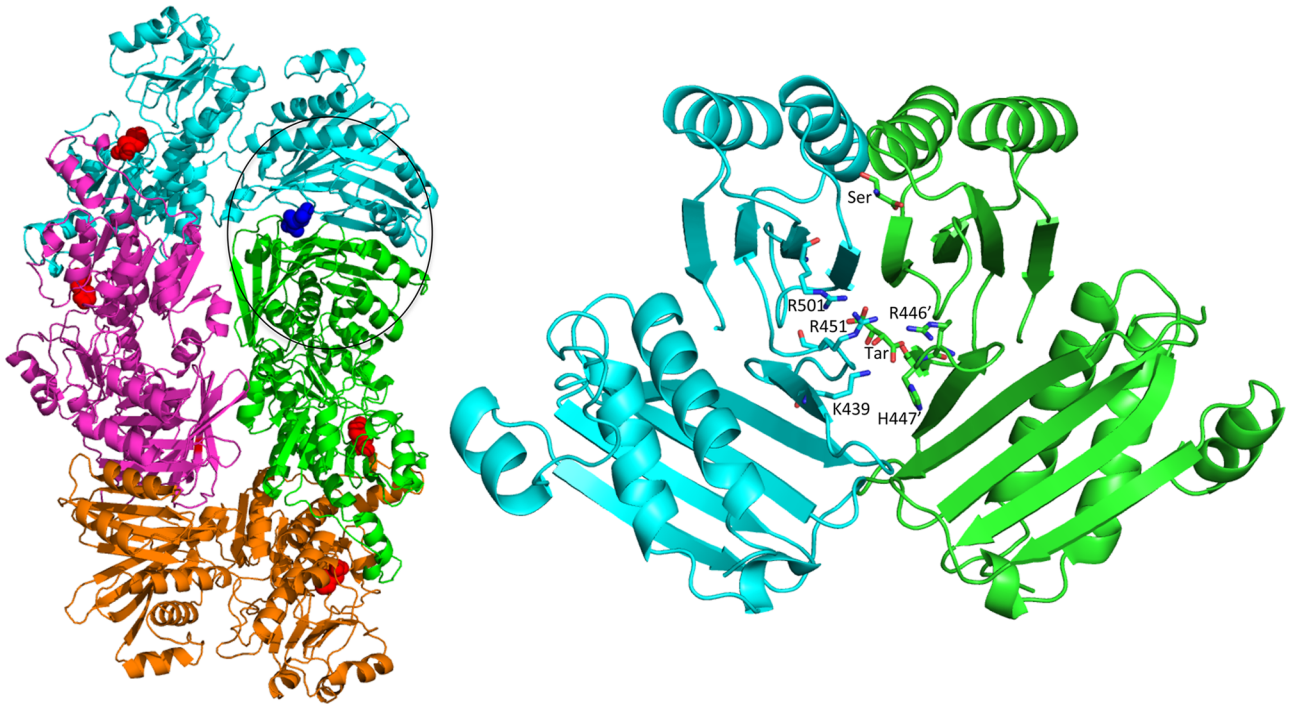

Figure 1. Structure of *mt*PGDH and the ASB−ACT domain interface of *M. tuberculosis* PGDH. At the left is shown the structure of *mt*PGDH from PDB entry 1YGY. Each subunit is displayed in a different color. His 280 at the active site is colored red. One ASB−ACT domain interface is highlighted by the oval, and the tartrate molecule is colored blue. At the right is shown the highlighted ASB−ACT domain interface expanded and reoriented to show the bound serine (Ser) and tartrate (Tar) molecules as well as the residues that bind the tartrate molecule (K439, R446′, H447′, R451, and R501). Only one site per dimer is shown for the sake of clarity.

dx.doi.org/10.1021/bi500469d | *Biochemistry* 2014, 53, 4239−4249

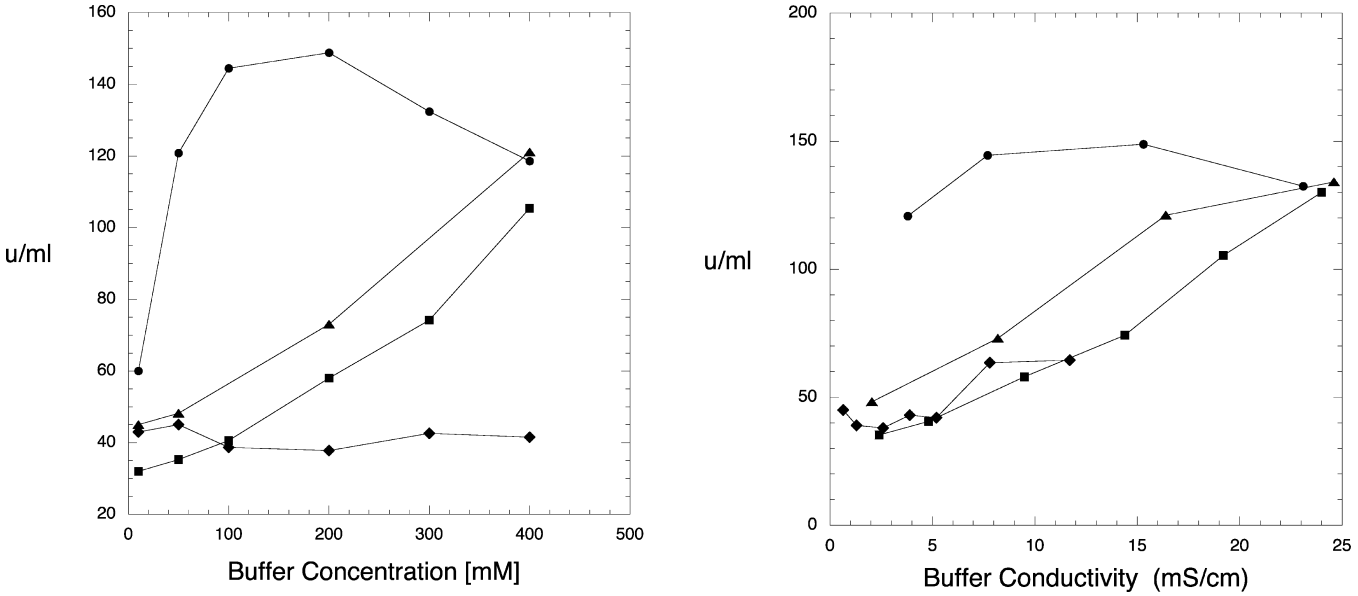

Figure 2. Activity of *mt*PGDH plotted vs increasing buffer concentration (left) and conductivity (right). Potassium phosphate (●), potassium acetate (▲), MOPS (◆), and Tris (■) were used as buffers (all at pH 7.0). The enzyme concentration was the same in all assays. Conductivity is expressed as millisiemens per centimeter. Data are represented by symbols, and lines have been interpolated between each point.

METHODS

*mt*PGDH was expressed with a hexahistidine tag at the amino terminus by placing the coding sequence into the 5′ BamHI site in pSV281 and expressed in BL21 DE3 cells. Cells were grown in Luria-Bertani medium at 30 or 37 °C, and expression was induced with 5 mM IPTG when the absorbance at 600 nm reached 0.5−0.7. The cells were harvested when the A_{600} was between 1 and 3. Cells were collected by centrifugation and suspended in a buffer that was either 50 mM MOPS or 200 mM potassium phosphate (each at pH 7.0). Cells were lysed by sonication in the presence of 0.16 mg/mL lysozyme, stirred for 10−20 min, and treated with 5 mg of DNAase. The supernatant was recovered after centrifugation, and the enzymes were purified using a Talon cobalt-based immobilized metal affinity column employing standard procedures. Buffer exchange was performed either with dialysis or with ultrafiltration using Amicon Ultra spin columns with a 10 kDa molecular weight cutoff. Enzyme activity was measured in the specified buffer with PHP and NADH as substrates by following the change in absorbance at 340 nm. Standard assay concentrations, except where otherwise indicated, were 275 μM NADH and 250 μM PHP. Because different buffer conditions produced different levels of activity, the assays of size exclusion chromatography (SEC) fractions were performed at an intermediate level of 150 μM PHP. One unit of enzyme activity is defined as the conversion of 1 nmol of NADH/min. NADH, PHP, and all buffers were from Sigma Chemical Co.

The six-His tag was removed from the protein by cleavage with tobacco etch virus (TEV) protease, containing a six-His tag and an S219V mutation,[16] at a protein:protease ratio of 20:1 (w/w) in 100 mM potassium phosphate buffer (pH 7.0), 4 mM β-mercaptoethanol, and 10% glycerol at room temperature for 4−6 h. β-Mercaptoethanol and glycerol were removed by overnight dialysis against 100 mM potassium phosphate buffer (pH 7.0). TEV protease and the cleaved six-His tag were removed from the protein when the mixture was passed through a cobalt metal affinity column. The wash-through, containing the cleaved protein, was recovered and concentrated by ultrafiltration. The characteristics of the enzyme with and without the six-His tag were the same kinetically and associatively.

Buffer conductivity was measured with an Orion 4 Star conductivity meter with Orion standards from Thermo Electron Corp. Conductivity was measured and expressed in units of millisiemens per centimeter. Size exclusion chromatography was performed with a 1.6 cm × 115 cm column of Sephacryl S300 HR. Samples were loaded in a volume of 1 mL at a nominal concentration of 50 μM, and 4 min fractions were collected at a flow rate of approximately 0.4 mL/min. The column was calibrated with protein standards, and the elution position was expressed as the volume at the apex of the absorbance trace. Blue dextran was used to determine the void volume, V_0. Chromatography was performed at least in duplicate under each condition, and elution positions were within 0.5 mL.

Gel electrophoresis was performed with precast 7.5% Bio-Rad Mini Protean gels in the presence or absence of SDS. Gels were stained with Coomassie Blue. All buffers were as recommended by the manufacturer.

Plots of activity versus substrate concentration were fit to a general equation for partial or complete substrate inhibition[17]

$$v = \frac{V_m + V_i([S]/K_i)}{1 + K_m/[S] + [S]/K_i} \quad (1)$$

where v is the velocity at substrate concentration [S], V_m is the maximal velocity, K_m is the apparent Michaelis constant, V_i is the maximal inhibited velocity, and K_i is the inhibition constant.

When complete inhibition is observed, $V_i = 0$, and the equation reduces to the standard equation for complete substrate inhibition

$$v = \frac{V_m}{1 + K_m/[S] + [S]/K_i} \quad (2)$$

dx.doi.org/10.1021/bi500469d | *Biochemistry* 2014, 53, 4239−4249

In the absence of substrate inhibition, plots of activity versus substrate concentration were fit to the Michaelis–Menten equation

$$v = \frac{V_m[S]}{K_m + [S]} \quad (3)$$

Plots of activity versus time were fit to the equation for one or more exponentials

$$Y = \sum_{i=n} A_i^{-k_{obs,i}t} + C \quad (4)$$

where Y is the activity at time t, $k_{obs,i}$ is the observed rate of the ith process, where n is the number of processes with an amplitude of A_i, and C is an offset value.

Serine inhibition is plotted as fractional activity, $(v_0 - v_i)/v_0$, versus serine concentration and fit to a Hill equation

$$I = [L]^n/(K_{0.5}{}^n + [L]^n) \quad (5)$$

where v_0 is the enzyme activity in the absence of inhibitor, v_i is the enzyme activity in the presence of inhibitor, [L] is the inhibitor ligand concentration, $K_{0.5}$ is the inhibitor concentration at half-maximal inhibition, and n is the Hill coefficient.

RESULTS

Effect of Buffer Components on Activity and Substrate Inhibition. It was previously reported that the activity and substrate inhibition observed with *mt*PGDH were sensitive to the ionic strength of the buffers used.[8] However, those studies employed only different concentrations of phosphate buffer. When buffers other than phosphate are used, it becomes apparent that the observed effects are not as much dependent on ionic strength as on the nature of the buffer salt itself. Figure 2 shows the effect of four different buffers on the activity of *mt*PGDH in terms of buffer concentration and buffer conductivity. While some effect of increasing conductivity is seen with other buffers, it is clear that optimal activity is obtained in phosphate buffer, especially at lower concentrations and conductivity, and reaches a maximum at 100–200 mM phosphate. Figure 3 shows typical curves of substrate inhibition of *mt*PGDH by PHP in the presence of 200 mM phosphate (pH 7.0) and 50 mM MOPS (pH 7.0). The substrate inhibition is much more pronounced in the MOPS buffer and the enzyme more active overall in the presence of phosphate.

The ability of L-serine to inhibit the catalytic activity of *mt*PGDH is also dependent on the nature of the buffer and relatively independent of the ionic strength. Figure 4 shows the inhibition of *mt*PGDH catalytic activity by L-serine in the presence of a cationic and three anionic buffers of equal conductivity (~10 mS/cm). L-Serine is least effective in the cationic Tris buffer with an IC_{50} for L-serine of 1573 ± 74 μM. The anionic buffers are all more effective with IC_{50} values of 798 ± 40, 378 ± 23, and 21 ± 1 μM for Hepes, acetate, and phosphate buffer, respectively. Because the buffers are all of equal ionic strength, these data demonstrate a preference or selectivity for the nature of the anion, with phosphate being much more effective than the others. Note that throughout the text, the enzyme forms whose catalytic activity is inhibited by low micromolar levels of L-serine will be described as being sensitive to L-serine. Those that are not significantly inhibited until L-serine levels are at millimolar concentrations are described as being insensitive.

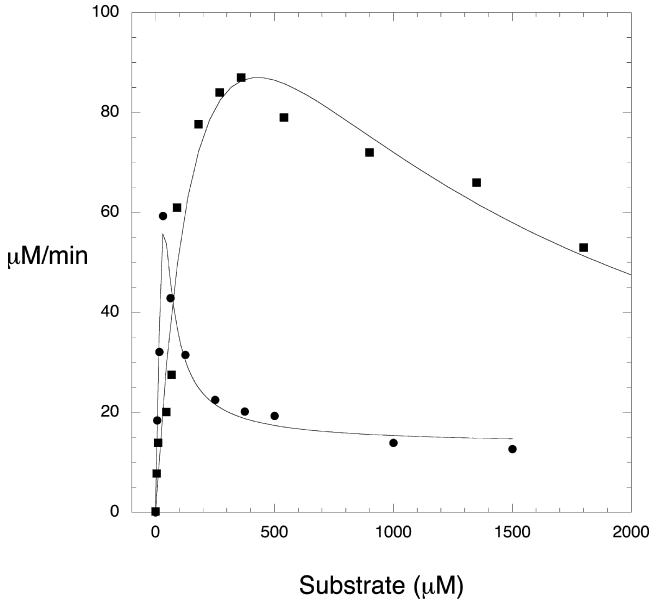

Figure 3. Substrate inhibition of *mt*PGDH. The activity of *mt*PGDH is measured as a function of increasing PHP concentration in 100 mM MOPS (pH 7.0) (●) and 100 mM potassium phosphate (pH 7.0) (■). Data are represented by symbols and are fit to eq 1.

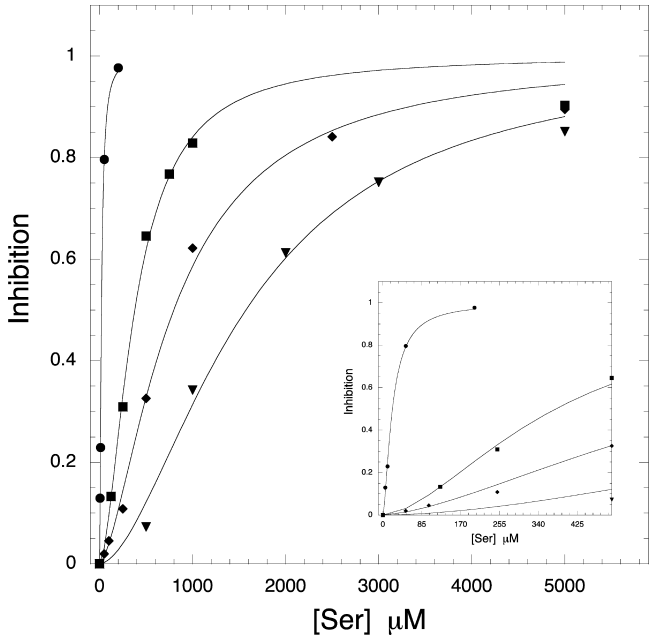

Figure 4. Inhibition of *mt*PGDH by L-serine in different buffers. The fractional inhibition of catalytic activity is plotted vs L-serine concentration. Potassium phosphate (●), potassium acetate (■), MOPS (◆), and Tris (▼) that were all adjusted to an equal conductivity of 10 mS/cm at pH 7.0 were used as buffers. The inset shows an expanded scale from 0 to 500 μM L-serine. Data are represented by symbols and are fit to eq 5.

Specificity for Phosphate. The selectivity for phosphate in enhancing the activity of *mt*PGDH and increasing its sensitivity to L-serine was further tested by analyzing the kinetic characteristics of the enzyme in 200 mM pyrophosphate buffer (pH 7.0) and 200 mM triphosphate buffer (pH 7.0). The results (Figure S1 of the Supporting Information) show a remarkable preference for phosphate as far as the ability of L-

dx.doi.org/10.1021/bi500469d | *Biochemistry* 2014, 53, 4239–4249

serine to inhibit catalytic activity is concerned. *mt*PGDH showed low micromolar sensitivity to L-serine in phosphate buffer, while that in pyrophospate and triphosphate buffer was significantly reduced and did not reach saturation even at 1 mM L-serine. The conductivity of the buffers was 25, 59, and 38 mS/cm for phosphate, pyrophosphate, and triphosphate, respectively. Therefore, the effect could not be attributed to a difference in buffer conductivity because both polyphosphate buffers have a conductivity slightly higher than that of phosphate, and the maximal conductivity difference was only approximately 2-fold for pyrophosphate and even smaller for triphosphate. Furthermore, the enzyme showed increased activity in pyrophosphate and triphosphate buffers at higher substrate concentrations. When the buffer concentration dependence of enzyme activity in phosphate and triphosphate is compared, the enzyme is clearly much more active in triphosphate, particularly at low concentrations (Figure S2 of the Supporting Information).

Evidence for Multiple Forms of *mt*PGDH. It was previously reported that *mt*PGDH lost activity upon dilution but that this could be prevented by increasing the phosphate concentration of the dilution buffer.[8] Interestingly, a re-examination of that data (Figure 5) shows that the plot of the loss of activity fits better to a double-exponential function than a single-exponential function. This observation suggests that there are at least two species present that dissociate with discernible inactivation constants, k_{inact}.

Native gels of *mt*PGDH dialyzed against either MOPS or phosphate buffer also provide evidence of more than one form of the enzyme (Figure S3 of the Supporting Information). *mt*PGDH from MOPS buffer shows at least four bands while that from phosphate shows mainly a single band. These bands likely represent monomer, dimer, tetramer, and a higher-order multimer, with the dark, main band from the phosphate sample corresponding to the tetramer.

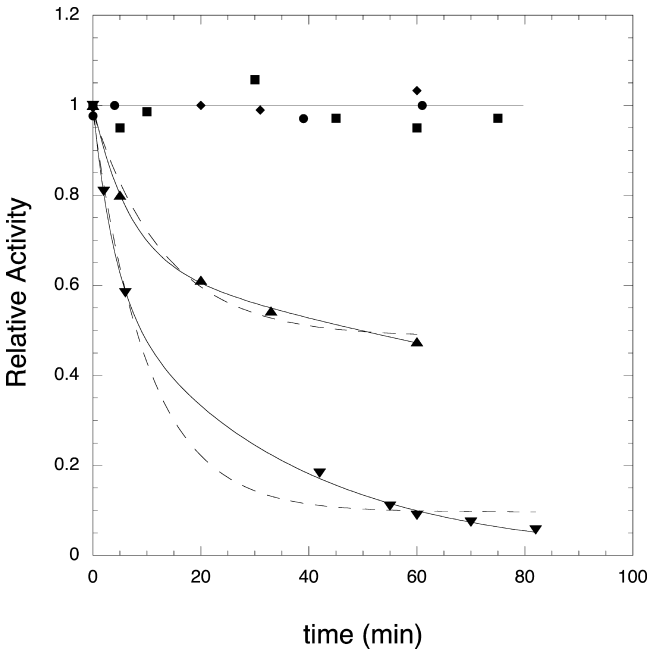

Figure 5. Effect of dilution on the activity of *mt*PGDH as a function of time and phosphate concentration. The data were taken from ref 8 and fit to a single-exponential (– – –) or double-exponential (—) function (eq 4). The enzyme is diluted at time zero from 200 mM potassium phosphate buffer (pH 7.5) and assayed at increasing times after dilution: 1/100 dilution in 200 mM potassium phosphate (pH 7.5) (●), 1/500 dilution in 200 mM potassium phosphate (pH 7.5) (■), 1/10 dilution in 20 mM potassium phosphate (pH 7.5) (◆), 1/100 dilution in 20 mM potassium phosphate (pH 7.5) (▲), and 1/500 dilution in 20 mM potassium phosphate (pH 7.5) (▼).

Size exclusion chromatography of *mt*PGDH in 50 mM MOPS buffer (pH 7.0), 200 mM phosphate buffer (pH 7.0), and 200 mM triphosphate buffer (pH 7.0) shows a distinct difference in the quaternary structure composition depending on the conditions (Figure 6). In 50 mM MOPS (Figure 6A), there are two distinct peaks with molecular weights of approximately 266400 and 136300. The closest calculated multimers to which these values correspond are a tetramer (calculated molecular weight of 226584) and a dimer (calculated molecular weight of 113292). However, both appear to run as if they are slightly larger (Figure 6D). Only the higher-molecular weight peak displays significant catalytic activity. In 200 mM phosphate (Figure 6B), two distinct peaks are also evident, but with molecular weights of approximately 519800 and 218900 that correspond to a 9-mer (calculated molecular weight of 509814) and a tetramer (calculated molecular weight of 226584), respectively. Although the larger peak has an apparent molecular weight closer to that of a 9-mer, it is most likely the association of two tetramers forming an octamer. The higher apparent molecular weight could be due to a more elongated shape with a slightly larger radius of gyration that would result from the association of two tetramers and that causes it to elute just a bit early. Both peaks display catalytic activity. In 200 mM triphosphate buffer (Figure 6C), there is a single peak with a molecular weight of approximately 110800 that corresponds to the dimer (calculated molecular weight of 113292). However, the peak is not completely symmetrical in that it appears to have a slight shoulder on the leading edge. This may be due to the presence of mixed dimer conformations, or there may be some tetramer present. Very interestingly, this peak displays a high level of catalytic activity, whereas the dimer peak observed in MOPS buffer (Figure 6A) does not. Figure 6D shows an overlay of the absorbance profiles from each condition. The overlay clearly shows that both peaks in MOPS buffer elute ahead of the elution position that would strictly apply to a dimer and tetramer. This slightly earlier elution suggests an alternate conformation with a slightly increased radius of gyration. Overall, the data suggest a scenario in which there are multiple ligand inducible equilibria. This is summarized in Figure 7 and Table 1.

The production of an active dimer by triphosphate was unexpected and prompted a closer look at the effect of triphosphate concentration. Figure 8 shows that as the triphosphate concentration increases, multimers that correspond most closely to the calculated tetramer molecular weight of 226584 elute progressively later in the SEC column. In 10, 50, and 100 mM triphosphate (pH 7.0), the peaks correspond to molecular weights of 278100, 239900, and 195000, respectively. This indicates that triphosphate has the effect of decreasing the hydrodynamic volume of the tetramer, and eventually, dissociation to a dimer occurs.

Size exclusion chromatography in the presence of 1 M tartrate, the condition that produced the published crystal structures, was unsuccessful because long-term exposure to the buffer caused the protein to precipitate on the column.

Effect of Tartrate on Catalytic Activity and Substrate Inhibition. If substrate and tartrate interact at the same site to

dx.doi.org/10.1021/bi500469d | *Biochemistry* 2014, 53, 4239–4249

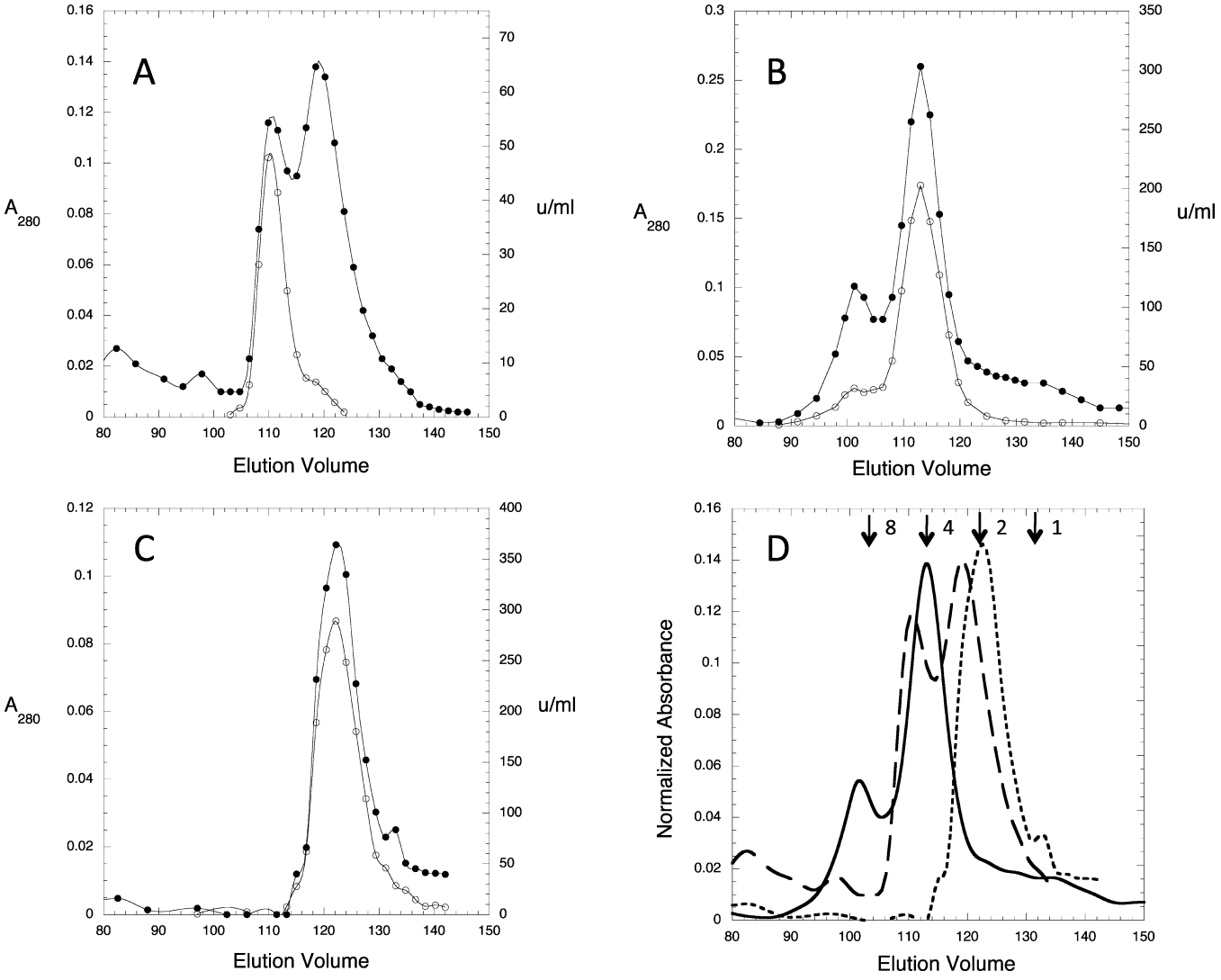

Figure 6. Size exclusion chromatography of *mt*PGDH. *mt*PGDH in the indicated buffer was applied to a 1.6 cm × 115 cm column of Sephacryl S-300 HR equilibrated with the same buffer at a flow rate of 0.4 mL/min. The absorbance at 280 nm (●) and the activity in units per milliliter (○) are plotted vs elution volume. The lines were interpolated through each data point using Kaleidograph: (A) 50 mM MOPS (pH 7.0), (B) 200 mM phosphate (pH 7.0), and (C) 200 mM triphosphate (pH 7.0). (D) Overlay of absorbance profiles from panels A (– – –), B (—), and C (···). The expected elution positions of the monomer, dimer, tetramer, and octamer are indicated.

inhibit the enzyme activity, tartrate should have a measurable effect on the substrate inhibition profile. Figure 9 shows plots of the enzyme activity versus substrate concentration in the presence and absence of varying amounts of sodium tartrate in 50 mM MOPS (pH 7.0). This range was chosen because the concentration present in the buffer used for crystallization of the published structure was 1 M. While the typical substrate inhibition profile is seen in the absence of tartrate, the plot with 0.25 M tartrate shows significantly less substrate inhibition, and the level decreases even further at higher tartrate concentrations. Furthermore, at low substrate concentrations, the activity in the presence of tartrate decreases as the tartrate concentration increases. In Figure 10, the effect of increasing tartrate concentration is shown at two substrate concentrations, 60 and 150 μM. A concentration of 60 μM was chosen because it is the concentration at which the enzyme displays maximal activity in MOPS buffer. At 150 μM PHP, the enzyme activity is reduced almost 3-fold (see Figure 3). In MOPS buffer, there is an initial activation of the enzyme activity that is much more pronounced at the higher substrate concentration. In phosphate and triphosphate buffers, the activation is not seen, and there is only a gradual decrease in activity as the tartrate concentration increases. The activation phase can be interpreted as tartrate competing with the substrate at the ASB–ACT domain site where it relieves substrate inhibition. The relative effect is larger for the higher substrate concentration because the initial level of inhibition is greater. This effect is blocked by the presence of phosphate and triphosphate, presumably because they interact at the same site. The gradual decrease in activity at higher concentrations may be due to a competitive substrate inhibition at the active site as depicted in Scheme 1.

■ DISCUSSION

This investigation clearly shows that phosphate ion greatly increases the sensitivity of *mt*PGDH to inhibition by L-serine. Furthermore, the closely related pyrophosphate and triphosphate molecules cannot replace phosphate in this respect, although they act similarly to phosphate in overcoming substrate inhibition.

dx.doi.org/10.1021/bi500469d | *Biochemistry* 2014, 53, 4239–4249

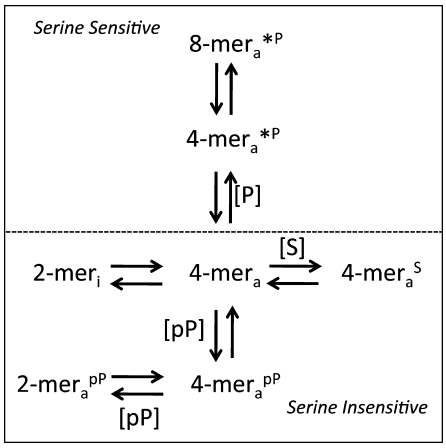

Figure 7. Equilibrium model of *mt*PGDH. The multimer equilibrium of *mt*PGDH as deduced from size exclusion chromatography analysis is depicted. The association state is indicated as *n*-mers. Reagents are indicated as [P] for phosphate, [pP] for polyphospahte, and [S] for substrate. The superscripts indicate bound ligands. An asterisk indicates a serine sensitive alternative conformation. A subscript a indicates an active enzyme. A subscript i indicates an inactive enzyme. Species above the dotted line are sensitive to L-serine and those below the dotted line insensitive to L-serine.

Table 1. Summary of Quaternary Structure Forms of D-3-Phosphoglycerate Dehydrogenase from *M. tuberculosis*

enzyme form	condition	catalytic activity[a]	serine sensitivity
2-mer$_i$	50 mM MOPS	none	not applicable
4-mer$_a$	50 mM MOPS	medium (400)	very low
4-mer$_a^S$	50 mM MOPS and tartrate	low (200)	very low
4-mer$_a$*^{P}	200 mM phosphate	high (800)	high
8-mer$_a$*^{P}	200 mM phosphate	medium (300)	high
2-mer$_a^{pP}$	200 mM triphosphate	very high (1700)	very low

[a]The number in parentheses is the average relative specific activity expressed as units per A_{280}.

The effect of phosphate ion concentration on the activity of *mt*PGDH was noted previously,[8] but its significance went unappreciated until the characteristics of the enzyme were also analyzed in other buffers. At the time, it had been noted that an increasing ionic strength could partially relieve substrate inhibition in rat PGDH,[12] and the effect with *mt*PGDH appeared to be similar. However, when *mt*PGDH was assayed in other buffers, it was noted that it displayed decreased activity (Figure 2) and was much more susceptible to substrate inhibition (Figure 3) and was no longer inhibited by low micromolar levels of L-serine (Figure 4). This was the first indication that there may be something special about the phosphate ion and its interaction with *mt*PGDH. In contrast, the type 2 PGDH from *E. coli* (*ec*PGDH) does not show substrate inhibition, and its activity is not enhanced by phosphate.[18] Phosphate causes only a slight increase in the serine sensitivity of *ec*PGDH with the IC_{50} in the absence of phosphate still being approximately 10 μM, far more sensitive than *mt*PGDH in the absence of phosphate.

The first indication that phosphate played a role in stabilizing quaternary structure was the observation that higher concentrations of phosphate prevented the loss of activity due to dilution. When the decay curves were fit to exponential functions, it was noted that they fit much better to two

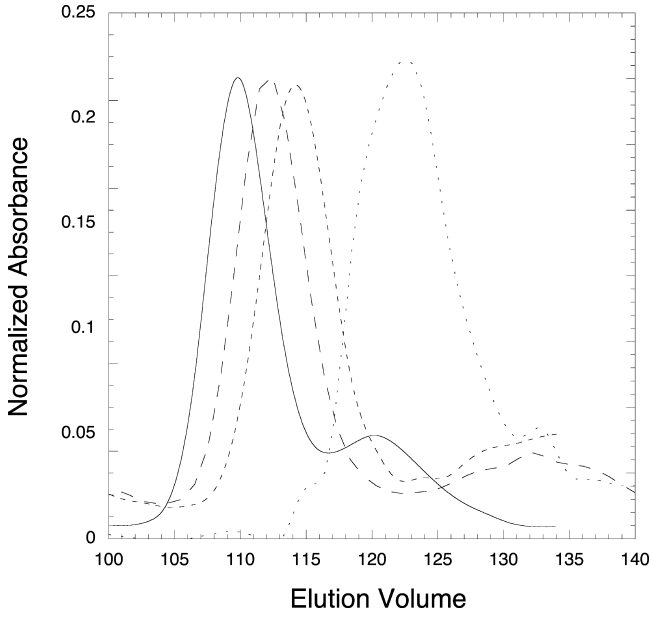

Figure 8. Comparative elution profiles of *mt*PGDH as a function of triphosphate concentration. The Sephacryl S-300 size exclusion chromatography elution profiles of *mt*PGDH in 10 mM triphosphate (pH 7.0) (—), 50 mM triphosphate (pH 7.0) (– – –), 100 mM triphosphate (pH 7.0) (---), and 200 mM triphosphate (pH 7.0) (···) are compared. The lines were interpolated through each data point using Kaleidograph. The data points are not shown.

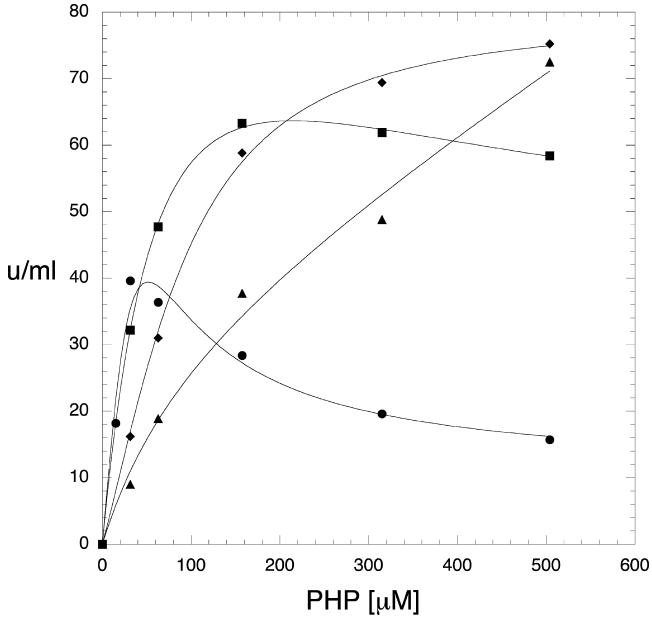

Figure 9. Substrate concentration-dependent activity profile of *mt*PGDH as a function of tartrate concentration. Equimolar amounts of *mt*PGDH are assayed as a function of PHP concentration in the absence (●) and presence of 0.25 M sodium tartrate (■), 0.5 M sodium tartrate (◆), and 1 M sodium tartrate (▲). All buffers were maintained at pH 7.0. Data are represented by symbols and are fit to eq 1.

exponentials than a single exponential, indicating that at least two forms of active enzyme that dissociated with different rates were present. Native gels of *mt*PGDH that had been preincubated in MOPS buffer showed at least four forms that correlated to a monomer, a dimer, a tetramer, and a higher-

dx.doi.org/10.1021/bi500469d | *Biochemistry* 2014, 53, 4239−4249

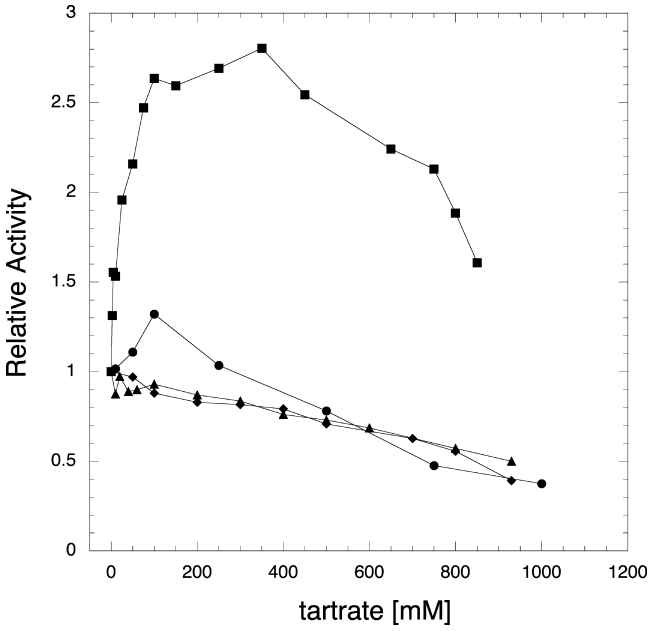

Figure 10. Tartrate concentration dependence as a function of substrate concentration and the presence of phosphate and triphosphate. First, the tartrate concentration dependence of activity is plotted in the presence of 60 (●) and 150 μM PHP (■) in 50 mM MOPS buffer (pH 7.0). Second, the tartrate concentration dependence of activity is plotted in the presence of 150 μM PHP in 200 mM phosphate buffer (pH 7.0) (◆) or 200 mM triphosphate buffer (pH 7.0) (▲).The lines are interpolated through each data point.

order multimer. *mt*PGDH that had been incubated in 100 mM phosphate was almost entirely a single band that was likely the tetramer. Size exclusion chromatography clearly demonstrates that the subunit conformation and association state of the enzyme change in response to phosphate and polyphosphate ion concentration. In the absence of phosphate, there is interconversion between an inactive dimer (2-mer$_i$) and an active tetramer (4-mer$_a$) that is not sensitive to L-serine inhibition. The tetramer association is weak because the dimer and tetramer can be resolved by SEC in almost equal amounts. The active tetramer can subsequently bind substrate (4-mer$_a^S$) at a second site that results in diminished catalytic activity through allosteric substrate inhibition. The active dimer or tetramer can be converted to an active, serine sensitive tetramer (4-mer$_a$*^{P}) by binding phosphate that can also associate with a serine sensitive octameric form (8-mer$_a$*^{P}). In the presence of triphosphate, there appears to be a concentration-dependent conformational compression of the tetrameric structure, and eventually, there is dissociation to an active dimer (2-mer$_a^{pP}$). None of the conformations in the presence of triphosphate are sensitive to L-serine. The serine sensitive and insensitive subunit conformations are likely to be different because there are small but measurable differences in the elution position of the multimers that contain them and there is a difference in the tendency of each respective dimer to form tetramers.

The crystal structure of *mt*PGDH revealed that tartrate, present in the crystallization buffer, participated in ionic interactions between two adjacent subunits. Tartrate is an analogue of the substrate, with both molecules having negatively charged groups at opposite ends of their structure. This observation led to the suggestion that the substrate could act as a natural noncovalent cross-linker and could be responsible for the substrate inhibition that was observed by acting allosterically.

Pyrophosphate and triphosphate contain two and three covalently linked phosphate groups, respectively, that would theoretically be able to interact with cationic residues on both sides of the dimer interface, similar to the case for tartrate, and form an effective ionic cross-link. Unexpectedly, both pyrophosphate and triphosphate decreased the level of substrate inhibition rather than enhancing it. In addition, triphosphate displayed an interesting alteration of the hydrodynamic size of the tetramer and eventually led to dissociation to an active dimer. Because the resultant dimer is active and an intact active site requires residues from adjacent subunits for activity,[15] the dimer is likely caused by dissociation at the ASB−ACT domain interface and not the active site interface. Because the ASB−ACT domain interface must be intact for ionic cross-linking to occur, the decreased level of substrate inhibition seen with pyrophosphate and triphosphate is consistent with substrate cross-linking being a primary cause of substrate inhibition. However, the data do not rule out the possibility that some competitive substrate inhibition may also be occurring as depicted in Scheme 1. This may be consistent with the observation that substrate inhibition is not completely abolished even in 200 mM phosphate buffer (Figure 3) at high substrate concentrations.

Phosphate ion would also be capable of binding at the anionic ASB−ACT domain interface and competing with the substrate for that site. In this case, the equilibrium shifts toward a tetrameric state that abolishes substrate inhibition and promotes sensitivity to inhibition by L-serine. The relative insensitivity to serine in other buffers also indicates that phosphate binding is required for serine to be an effective inhibitor. This is consistent with the observation that mutation of the ASB−ACT domain interface cationic residues to alanine decreases serine sensitivity and the level of substrate inhibition.[19] The sulfonic acid group found in MOPS will not substitute for phosphate.

This scenario is consistent with the "morpheein" model of quaternary structure dynamics that has been shown by Jaffe to exist with porphobilinogen synthase[20−22] and possibly with phenylalanine hydroxylase.[23] In the case of porphobilinogen synthase, there is an equilibrium between an active octamer and an inactive hexamer that form through interconversion of dimeric species of different conformations. In the case of phenylalanine hydroxylase, Jaffe has proposed that there is an equilibrium between alternate tetrameric structures that form from two different dimeric conformations. However, a main component of this model is that there is interconversion between dissociated species. Additional work will be required to demonstrate this directly for PGDH.

The available crystal structures for *mt*PGDH come from enzymes that were all crystallized in the absence of phosphate and the presence of 1 M tartrate and show a tartrate molecule bound at the ASB−ACT domain interface. As such, these structures are likely representative of the 4-mer$_a^S$ form that allosterically binds substrate. The slightly early eluting peaks found in the presence of MOPS buffer (Figure 6A,D) suggest that they may represent an altered conformation that has a radius of gyration slightly larger than those in the presence of phosphate (Figure 6B). If this is the case, then it is likely the consequence of a conformational change in the enzyme subunits and would be expected to provide a structure in the presence of phosphate ion that displays significant differences

dx.doi.org/10.1021/bi500469d | *Biochemistry* 2014, 53, 4239−4249

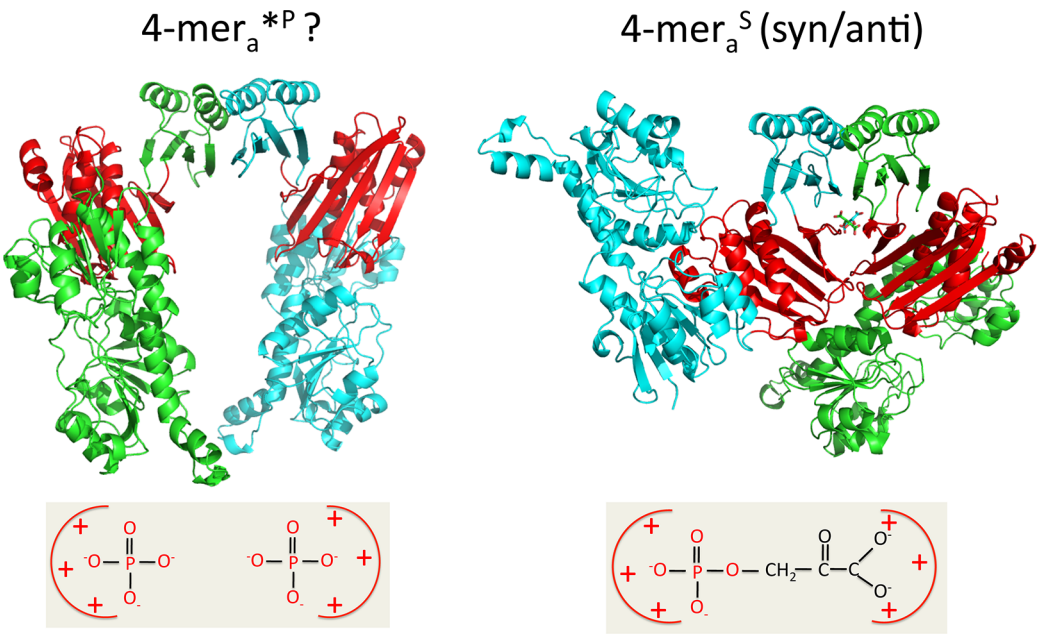

Figure 11. Theoretical model of interaction of phosphate and substrate at the ASB−ACT domain interface. At the right is shown the structure of the *mt*PGDH *syn*/*anti* dimer from PDB entry 3DC2 crystallized in MES buffer with 1 M tartrate. Below is an inexact diagram depicting how the substrate may interact electrostatically with both monomers at the dimer interface based on the binding of tartrate in the crystal structure. At the left is shown a theoretical depiction of a possible alternative conformation in the presence of phosphate. The dimer structure conserves the ACT domain contacts, but the ASB domains (red) are no longer in contact with each other. Rotation around a glycine residue in the strand between the ASB and ACT domains was required to prevent subunit contact. Below is an inexact diagram depicting how two phosphate ions may interact with the substrate and/or tartrate binding site to eliminate the cross-linking effect and possibly produce electrostatic repulsion between the ASB domains.

compared to the available X-ray structures. A hypothetical rendering of how that structure might look is also presented in Figure 11, which is intentionally exaggerated to illustrate the loss of the ASB domain interface interaction while the ACT domain interface is maintained so that serine binding can occur. In other words, the ASB domain interface is lost because the subunits assume a conformation that moves the domains apart. Furthermore, the ability of tartrate and phosphates to block inhibition by substrate that is associated with the cationic site at the ASB−ACT domain interface suggests that they may all interact at the same site.

The action of the small polyphosphates used in this study also suggests that they may play a physiological role in the regulation of serine synthesis. In effect, the interplay of phosphate and polyphosphate may represent a metabolic switch between a higher-activity enzyme that is insensitive to feedback inhibition by serine and a lower-activity enzyme that is sensitive to feedback inhibition by serine. Inorganic polyphosphates are found in plants, animals, and bacteria, including *M. tuberculosis*, play a role in bacterial survival, and are required for virulence in many bacteria.[24−28] In addition to "acid-insoluble" long chain polyphosphates, "acid-soluble" short chain polyphosphates are found in bacterial cells.[24] Among other things, polyphosphates accumulate in response to a deficiency of amino acids.[29,30] In addition, polyphosphonucleotides such as the guanosine pentaphosphate and tetraphosphate, (p)ppGpp, regulate numerous cellular processes, such as virulence and persistence[31,32] and cause an inhibition of RNA synthesis in which there is a shortage of amino acids. It also causes the upregulation of genes for amino acid biosynthesis and uptake,[33] the overall effect being to conserve what amino acids there are and to increase the size of the amino acid pool. The demonstration that polyphosphates interact with *mt*PGDH to produce a very active enzyme that is resistant to inhibition by L-serine may provide a mechanism for the efficient production of L-serine that is not subject to feedback regulation by increasing levels of serine. Obviously, much more work will need to be done in this area to explore this hypothesis.

As far as we know, the phosphate induction of serine sensitivity is unique to certain pathogenic *Mycobacterium* species among organisms that contain type 1 PGDH enzymes. The reason why phosphate ion is required for the induction of greater sensitivity to L-serine concentrations in pathogenic mycobacteria is not known. In addition to its incorporation into proteins, L-serine is central to the production of many other metabolites such as glycine, L-cysteine, L-methionine, L-tryptophan, phosphatidylserine, sphingolipids, purines, porphyrins, and glyoxalate. As the major precursor to glycine, it contributes the one-carbon unit (C1) that is the donor in methylation reactions mediated by derivatives of tetrahydrofolate (THF) and *S*-adenosylmethionine (SAM). The last step in the serine biosynthetic pathway is the conversion of phosphoserine to serine with the liberation of inorganic phosphate. As serine is converted into other metabolites, phosphate concentrations may build up to the point that PGDH, the first enzyme in the pathway, becomes increasingly sensitive to L-serine in a feedback mechanism that balances the use of phosphoglycerate from glycolysis with the production of serine metabolites. Without phosphate, serine concentrations may never reach the level needed for feedback inhibition, and glucose would continue to be depleted. If low levels of serine by itself were capable of effective feedback inhibition, the organism may become starved for the serine-derived metabolites. Why *mt*PGDH differs in this regard from other type 1 enzymes that are not inhibited by serine even in the presence of phosphate is not known, but it may be that this function has evolved to

dx.doi.org/10.1021/bi500469d | *Biochemistry* 2014, 53, 4239−4249

support the intracellular pathogenic lifestyle of the organisms and its relationship to its host metabolism.

How the levels of phosphate and polyphosphates reported here compare to the physiological levels that may be encountered in the organism is a valid consideration. As far as we can tell, the intracellular concentrations of phosphate and polyphosphates have not been reported for *M. tuberculosis*, and measuring the levels of metabolites is particularly problematic for the latent bacteria in the macrophage. In general, it is known that polyphosphates can act as a reservoir for phosphate and that polyphosphate pools can be as much as 30% of dry cell weight in some bacteria, i.e., *Acinetobacter johnsonii*.[24] In addition, the phenomenon of compartmentalized metabolism in prokaryotic cells can result in locally high concentrations of metabolites.[34,35]

In any case, this investigation has revealed a mechanism of allosteric quaternary structure dynamics in an important metabolic enzyme in *M. tuberculosis* that is modulated by physiologically relevant molecules. This may provide infectious *Mycobacterium* species with a unique metabolic advantage and may represent a metabolic target with future potential for antituberculosis research.

■ ASSOCIATED CONTENT

Supporting Information

Figures showing the level of enzyme activity in phosphate, pyrophosphate, and triphosphate buffers as well as a native gel of the enzyme in the presence and absence of phosphate. This material is available free of charge via the Internet at http://pubs.acs.org.

■ AUTHOR INFORMATION

Corresponding Author

*Department of Medicine and Department of Developmental Biology, Washington University School of Medicine, St. Louis, MO 63110. E-mail: ggrant@wustl.edu. Phone: (314) 362-3367. Fax: (314) 362-4698.

Notes

The authors declare no competing financial interest.

■ ACKNOWLEDGMENTS

We thank Eileen Jaffee for helpful discussions regarding the morpheein model and Christina Stallings for helpful discussions regarding the metabolism of *M. tuberculosis*.

■ ABBREVIATIONS

PGDH, D-3-phosphoglycerate dehydrogenase; *Mtb*, *M. tuberculosis*; *mt*PGDH, *M. tuberculosis* D-3-phosphoglycerate dehydrogenase; PHP, phosphohydroxypyruvate [also called hydroxypyruvic acid phosphate (HPAP)]; ACT, acronym for aspartate kinase, chorismate mutase, TyrA; ASB, acronym for allosteric substrate binding.

■ REFERENCES

(1) Walsh, D. A., and Sallach, H. J. (1966) Comparitive studies on the pathways for serine biosynthesis in animal tissues. *J. Biol. Chem. 241*, 4068−4076.

(2) Willis, J. E., and Sallach, H. J. (1964) The occurence of D-3-phosphoglycerate in animal tissue. *Biochim. Biophys. Acta 81*, 39−54.

(3) Rosenblum, I. Y., and Sallach, H. J. (1970) Purification and properties of wheat germ D-3-phosphoglycerate dehydrogenase. *Arch. Biochem. Biophys. 137*, 91−101.

(4) Slaughter, J. C., and Davies, D. D. (1975) 3-Phosphoglycerate dehydrogenase from seedlings of *Pisum sativum*. *Methods Enzymol. 41*, 278−281.

(5) Ali, V., Hashimoto, T., Shigeta, Y., and Nozaki, T. (2004) Molecular and biochemical characterization of D-phosphoglycerate dehydrogenase from *Entamoeba histolytica*: A unique enteric protozoan parasite that possesses both phosphorylated and nonphosphorylated serine metabolic pathways. *Eur. J. Biochem. 271*, 2670−2681.

(6) Grant, G. A. (2012) Contrasting catalytic and allosteric mechanisms for phosphoglycerate dehydrogenases. *Arch. Biochem. Biophys. 519*, 175−185.

(7) Grant, G. A. (2006) The ACT Domain: A small molecule binding domain and its role as a common regulatory element. *J. Biol. Chem. 281*, 33825−33829.

(8) Dey, S., Hu, Z., Xu, X. L., Sacchettini, J. C., and Grant, G. A. (2005) D-3-Phosphoglycerate dehydrogenase from *Mycobacterium tuberculosis* is a link between the *Escherichia coli* and mammalian enzymes. *J. Biol. Chem. 280*, 14884−14891.

(9) Burton, R. L., Chen, S., Xu, X. L., and Grant, G. A. (2009) Role of the anion-binding site in catalysis and regulation of *Mycobacterium tuberculosis* D-3-phosphoglycerate dehydrogenase. *Biochemistry 48*, 4808−4815.

(10) Xu, X. L., Chen, S., and Grant, G. A. (2011) Kinetic, mutageneic and structural homology analysis of L-serine dehydratase from *Legionella pneumophila*. *Arch. Biochem. Biophys. 515*, 28−36.

(11) Grant, G. A. (2012) Kinetic evidence of a non-catalytic substrate binding site that regulates activity in *Legionella pneumophila* L-serine dehydratase. *Biochemistry 51*, 6961−6967.

(12) Achouri, Y., Rider, M. H., Van Schaftingen, E., and Robbi, M. (1997) Cloning, sequencing and expression of rat liver 3-phosphoglycerate dehydrogenase. *Biochem. J. 323*, 365−370.

(13) Burton, R. L., Hanes, J. W., and Grant, G. A. (2008) A stopped flow transient kinetic analysis of substrate binding and catalysis in *Escherichia coli* to D-3-phosphoglycerate dehydrogenase. *J. Biol. Chem. 283*, 29706−29714.

(14) Dey, S., Burton, R. L., Grant, G. A., and Sacchettini, J. C. (2008) Structural analysis of substrate and effector binding in *Mycobacterium tuberculosis* D-3-phosphoglycerate dehydrogenase. *Biochemistry 47*, 8271−8282.

(15) Dey, S., Grant, G. A., and Sacchettini, J. C. (2005) Crystal structure of *Mycobacterium tuberculosis* D-3-phosphoglycerate dehydrogenase. *J. Biol. Chem. 280*, 14892−14899.

(16) Kapust, R. B., Routzahn, K. M., and Waugh, D. S. (2002) Processive degradation of nascent polypeptides, triggered by tandem AGA codons, limits the accumulation of recombinant TEV protease in *Escherichia coli* BL21(DE3). *Protein Expression Purif. 24*, 61−70.

(17) LiCata, V. J., and Allewell, N. M. (1997) Is substrate inhibition a consequence of allostery in aspartate transcarbamylase? *Biophys. Chem. 64*, 225−234.

(18) Grant, G. A., Xu, X. L., Hu, Z., and Purvis, A. R. (1999) Phosphate ion partially relieves the cooperativity of effector binding in D-3-phosphoglycerate dehydrogenase without altering the cooperativity of inhibition. *Biochemistry 38*, 16548−16552.

(19) Burton, R. L., Chen, S., Xu, X. L., and Grant, G. A. (2007) A novel mechanism for substrate inhibition in *Mycobacterium tuberculosis* D-3-phosphoglycerate dehydrogenase. *J. Biol. Chem. 282*, 31517−31524.

(20) Breinig, S., Kervinen, J., Stith, L., Wasson, A. S., Fairman, R., Wlodawer, A., Zdanov, A., and Jaffe, E. K. (2003) Control of tetrapyrrole biosynthesis by alternate quaternary forms of orphobilinogen synthase. *Nat. Struct. Biol. 10*, 757−763.

(21) Jaffe, E. K. (2005) Morpheeins: A new structural paradigm for allosteric regulation. *Trends Biochem. Sci. 30*, 490−497.

(22) Jaffe, E. K., and Lawrence, S. H. (2012) Allostery and the dynamic oligomerixation of porphobilinogen synthase. *Arch. Biochem. Biophys. 519*, 144−153.

(23) Jaffe, E. K., Stith, L., Lawrence, S. H., Andrake, M., and Dunbrack, R. L., Jr. (2013) A new model for allosteric regulation of

phenylalanine hydroxylase: Implications for disease and therpeutics. *Arch. Biochem. Biophys. 530*, 73−82.
(24) Achbergerová, L., and Nahálka, J. (2011) Polyphosphate: An ancient energy source and active metabolic regulator. *Microb. Cell Fact. 10*, 63.
(25) Singh, R., Singh, M., Arora, G., Kumar, S., Tiwari, P., and Kidwai, S. (2013) Polyphosphate deficiency in *Mycobacterium tuberculosis* is associated with enhanced drug susceptibility and impaired growth in guinea pigs. *J. Bacteriol. 195*, 2839−2851.
(26) Rashid, M. H., Runbaugh, K., Passador, L., Davies, D. G., Hamood, A. N., Iglewski, B. H., and Kornberg, A. (2000) Polyphosphate kinase is essential for biofilm development, quorum sensing, and virulence of *Pseudomonas aeruginosa*. *Proc. Natl. Acad. Sci. U.S.A. 97*, 9636−9641.
(27) Kornberg, A., Rao, N. N., and Ault-Riché, D. (1999) Inorganic polyphosphate: A molecule of many functions. *Annu. Rev. Biochem. 68*, 89−125.
(28) Rifat, D., Bishai, W. R., and Karakousis, P. C. (2009) Phosphate depletion: A novel trigger for *Mycobacterium tuberculosis* persistence. *J. Infect. Dis. 200*, 1126−1135.
(29) Rao, N. N., and Kornberg, A. (1996) Inorganic polyphosphate supports resistance and survival of stationary-phase *Escherichia coli*. *J. Bacteriol. 178*, 1394−1400.
(30) Rao, N. N., and Kornberg, A. (1999) Inorganic polyphosphate regulates responses of *Escherichia coli* to nutritional stringencies, environmental stresses and survival in the stationary phase. *Prog. Mol. Subcell. Biol. 23*, 183−195.
(31) Haralalka, S., Nandi, S., and Bhadra, R. K. (2003) Mutation in the relA gene of *Vibrio cholerae* affects in vitro and in vivo expression of virulence factors. *J. Bacteriol. 185*, 4672−4682.
(32) Klinkenberg, L. G., Lee, J. H., Bishai, W. R., and Karakousis, P. C. (2010) The stringent response is required for full virulence of *Mycobacterium tuberculosis* in guinea pigs. *J. Infect. Dis. 202*, 1397−1404.
(33) Srivatsan, A., and Wang, J. D. (2008) Control of bacterial transcription, translation and replication by (p)ppGpp. *Curr. Opin. Microbiol. 11*, 100−105.
(34) Eoh, H., and Rhee, K. Y. (2014) Allostery and compartmentalization: Old but not forgotten. *Curr. Opin. Microbiol. 18*, 23−29.
(35) Carvalho, L. P., Fischer, S. M., Marrero, J., Nathan, C., Ehrt, S., and Rhee, K. Y. (2010) Metabolomics of *Mycobacterium tuberculosis* reveals compartmentalized co-catabolism of carbon substrates. *Chem. Biol. 17*, 1122−1131.